https://doi.org/10.5194/egusphere-2026-2512
Preprint. Discussion started: 13 May 2026

Urbanization drives coupled shifts in soil-carbon stocks, sources, and stability across natural and restored mangroves and tidal flats

Minde Huang[1,2], Fen Guo[1,2,*], Xueqin Gao[3], Xiaoguang Ouyang[4], Yuan Zhang[1,2]

[1]Guangdong Basic Research Center of Excellence for Ecological Security and Green Development, Guangdong Provincial Key Laboratory of Water Quality Improvement and Ecological Restoration for Watersheds, School of Ecology, Environment and Ocean, Guangdong University of Technology, Guangzhou 510006, China

[2]Guangdong Provincial Observation and Research Station for Social-Natural Complex Ecosystems in Haizhu Wetlands, 510399, Guangzhou, China

[3]Experimental Marine Ecology Laboratory, Department of Biological Sciences, National University of Singapore, Block S3, 16 Science Drive 4, 117558 Singapore

[4]Research Centre of Ecology & Environment for Coastal Area and Deep Sea, Southern Marine Science and Engineering Guangdong Laboratory (Guangzhou), Guangzhou 511458, China

Correspondence to: Fen Guo (fen.guo@gdut.edu.cn)

Abstract. Urbanization reshapes coastal blue carbon, but its effects on how much carbon is stored, who supplies it, and how long it persists remain poorly integrated. We investigated natural and restored mangroves and adjacent tidal flats along an urbanization gradient, and quantified soil organic carbon stocks, burial from ^{210}Pb profiles, source composition using isotope end-member mixing, and stability from turnover metrics. Our results showed a coordinated triad response to urbanization. Carbon stocks and burial declined, sources shifted away from mangrove detritus toward planktonic and algal inputs, and turnover accelerated, lowering stability. Responses were habitat dependent and nonlinear. Natural mangroves in low urbanization settings maintained the highest sequestration with mangrove-dominated inputs and slower turnover. Restored stands and tidal flats showed steeper stock losses, stronger source substitution, and faster cycling under higher urban pressure. We introduced a triad framework that treats stocks, sources, and stability as coupled state variables along the urbanization gradient and identified two reproducible system states: carbon anchors in low urbanization natural mangroves and instability fronts in restored stands and tidal flats. Shifts in sources and stability precede stock losses, providing clear early warnings of urban impact. A simple diagnostic that combines connectivity and accretion with source composition and a composite stability index guides anchor protection and stability-first restoration. These results link urban growth to blue-carbon performance and define actionable thresholds for sustaining coastal carbon.

https://doi.org/10.5194/egusphere-2026-2512
Preprint. Discussion started: 13 May 2026

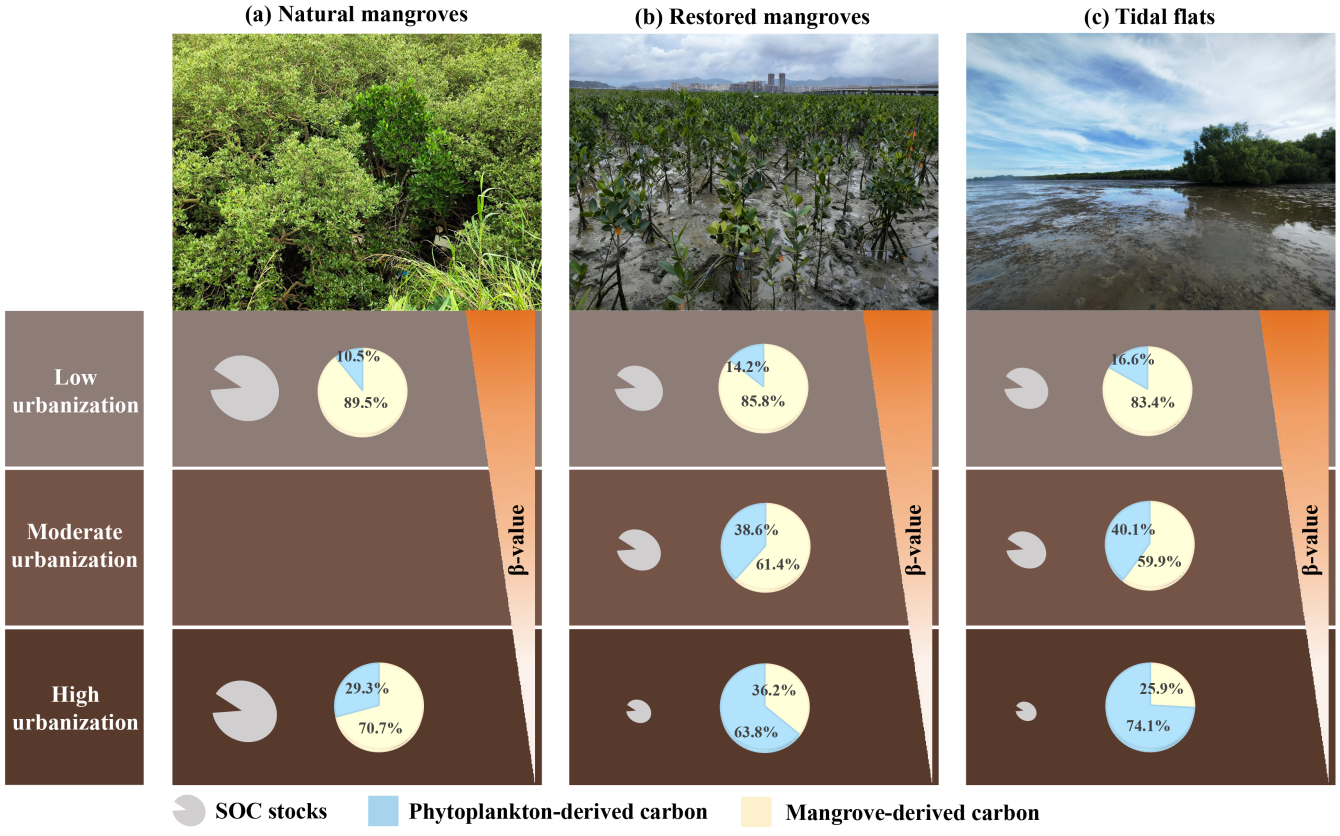

1 Introduction

Mangrove forests are among the most carbon-dense coastal ecosystems, with soils that store organic carbon over millennial timescales and make a disproportionate contribution to climate mitigation (Atwood et al., 2017; Liao et al., 2025). Globally, mangrove soils store an estimated 3.7–11.7 Pg C and bury 18.4–34.4 Tg C yr^{-1}, magnitudes that underscore their climate significance (Kauffman et al., 2020; Ouyang and Lee, 2020; Wang et al., 2023). As coastal populations expand, urbanization is increasingly reshaping hydrosedimentary regimes, nutrient and contaminant loads, and vegetation structure, which can alter how much carbon is stored and buried, where it comes from, and how securely it is retained (Branoff, 2017; Hao et al., 2024; Wei et al., 2024). A mechanism-based understanding is therefore essential to forecast blue-carbon persistence and to design restoration that rebuilds carbon quantity, source quality, and long-term stability.

Urbanization acts through coupled pathways that connect coastal physics to soil biogeochemistry. Reduced tidal connectivity and altered sediment supply change the quantity and depositional environment of organic matter entering soils (Hamilton and Friess, 2018; Kauffman et al., 2018; Wei et al., 2024). Concurrent nutrient enrichment and contaminants from sewage, aquaculture, and industry shift source quality and microbial processing, with consequences for decomposition and carbon

https://doi.org/10.5194/egusphere-2026-2512
Preprint. Discussion started: 13 May 2026

mineralization (Fu et al., 2023; Lee, 2016; Wu et al., 2024). These drivers jointly regulate the probability that incoming carbon becomes protected within mineral-associated organic matter and microaggregates, which determines the stability and turnover of soil carbon pools (Liu et al., 2024; Lovelock and Reef, 2020; Spivak et al., 2019). Although climate trends and local management can amplify or dampen these responses, we still lack a clear account of how urbanization reorganizes the coupled dimensions of quantity, quality, and stability along the explicit gradients.

Despite growing attention to mangroves in urban settings, most work on urban mangroves measures area change, bulk soil carbon, or burial in isolation (Ai et al., 2020; Branoff, 2017; Wei et al., 2024), with source apportionment and stability rarely evaluated in the same gradient-based design. This disconnect prevents attribution, because a decline in stocks can arise from reduced inputs or from weaker protection. Resolving the mechanism requires an integrated framework that links stocks and burial to indicators of source and stability along urbanization gradients, including the partitioning of particulate versus mineral-associated organic matter, the proportion of Fe or Al bound carbon, and thermal or radiocarbon metrics. Such alignment allows the limiting step to be identified and directly tests how urbanization reorganizes the coupled dimensions of quantity, source composition, and stability.

A second gap is the lack of gradient-based comparisons that span natural mangroves, restored mangroves, and adjacent unvegetated tidal flats. These habitats occupy distinct positions along the coastal carbon pathway. Tidal flats provide the unvegetated depositional baseline that integrates watershed and coastal inputs but lacks persistent plant-mediated protection (Lin et al., 2020; Wu et al., 2025). Restored mangroves capture assembly trajectories in which plant inputs, rhizosphere effects, and stabilization mechanisms are forming (Jimenez et al., 2021; Sun et al., 2024), and are therefore diagnostically sensitive to urban stressors. Natural mangroves provide the mature reference with sustained autochthonous inputs and a higher probability of mineral association that supports large and stable soil-carbon pools (Chen et al., 2018; Hong Tinh et al., 2020; Huang et al., 2025a). Without a three-habitat comparison across urbanization gradients, it is difficult to separate input limitation from protection failure or to evaluate when and where restoration can converge toward natural levels of stability.

To address these gaps, we conducted a gradient-based cross-ecosystem study that jointly evaluates carbon quantity, source quality, and stability in natural mangroves, restored mangroves, and adjacent unvegetated tidal flats across low, moderate, and high urbanization levels. Our objective was to elucidate how urbanization reshapes soil carbon dynamics in mangroves and their neighboring ecosystems by altering carbon input sources and stabilization pathways, thereby uncovering the mechanisms regulating blue carbon along an urbanization gradient. We test three hypotheses:

(H1) soil carbon stocks and burial rates decline with increasing urbanization intensity, with natural mangroves in low-urbanized areas maintaining higher storage and sequestration;

(H2) the composition of organic-carbon sources is more sensitive to urbanization in restored mangroves and tidal flats, whereas natural mangrove soils remain dominated by mangrove-derived inputs; and

https://doi.org/10.5194/egusphere-2026-2512
Preprint. Discussion started: 13 May 2026

(H3) under lower urbanization pressure, soil-carbon pools are more stable across habitats.

2 Methods

2.1 Study area

This study was conducted in three coastal cities in Guangdong Province, southern China: Zhanjiang, Shantou, and Huizhou. An urbanization gradient was established using four socioeconomic indicators, namely urban population proportion, non-agricultural population proportion, per capita disposable income of urban residents, and built-up area. Based on these indicators, Zhanjiang, Shantou, and Huizhou represent low, moderate, and high levels of urbanization, respectively (data source: http://tjnj.gdstats.gov.cn:8080/tjnj/2024/; Appendix A Table A1). These cities were located in different parts of Guangdong's coastline: Zhanjiang in the southwest (109°40′–110°58′E, 20°13′–21°57′N), Shantou in the east (116°14′–117°19′E, 23°02′–23°38′N), and Huizhou in the southeast (113°51′–115°28′E, 22°24′–23°57′N) (Fig. 1). The study area lies within the East Asian monsoon zone, characterized by a mean annual temperature of 22.1 °C and an average annual precipitation of 1,798.8 mm. In addition, annual sunshine duration increases from north to south, ranging from less than 1,500 hours to over 2,100 hours (data source: Guangdong Yearbook 2024).

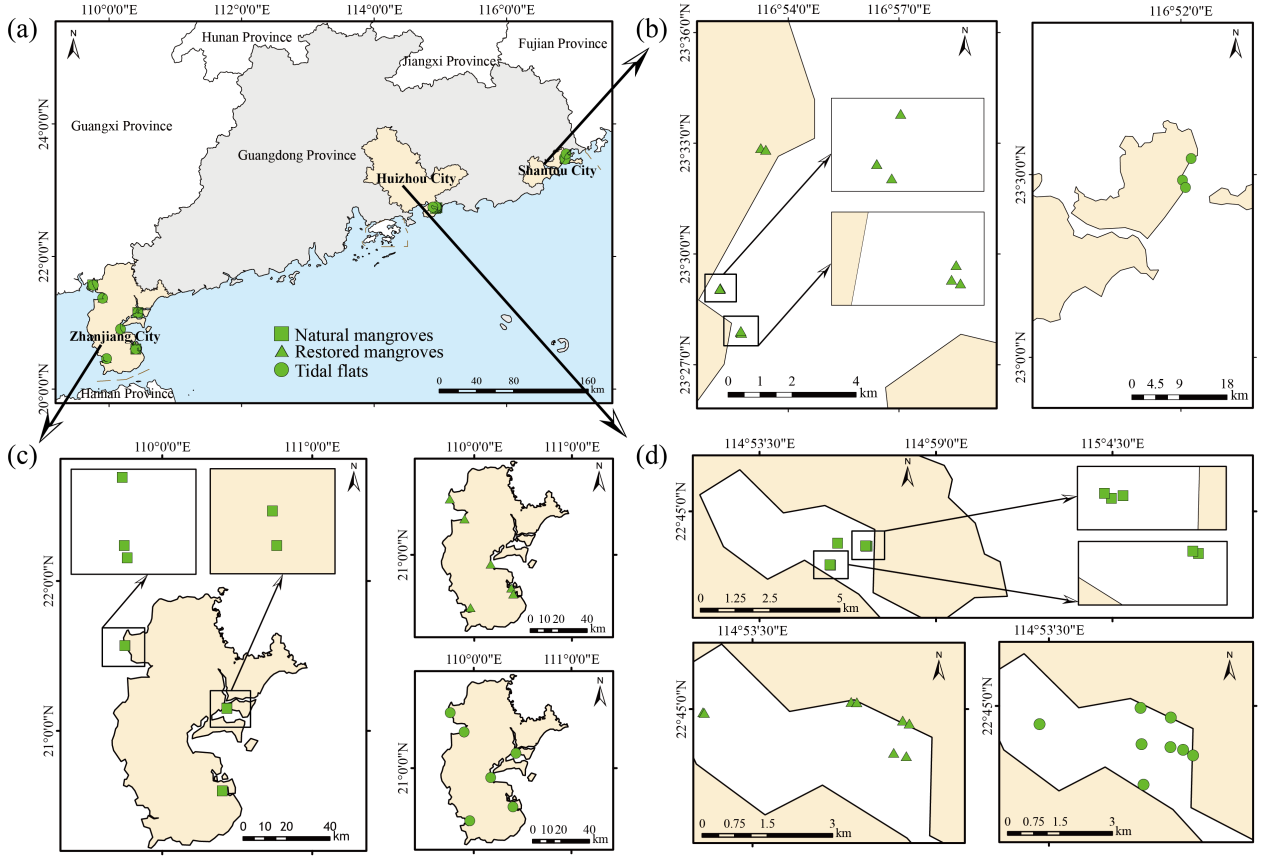

https://doi.org/10.5194/egusphere-2026-2512
Preprint. Discussion started: 13 May 2026

Figure 1. Location of sampling sites across high, moderate, and low urbanization gradients in southern China, showing natural mangroves, restored mangroves, and tidal flats.

Historically, the mangrove resources in these three regions were abundant. However, with the acceleration of urbanization, intensified human activities such as aquaculture, coastal engineering, and population growth have led to severe degradation of mangrove ecosystems (Kang et al., 2025; Tang et al., 2023). From 2020 to the end of April 2025, under government initiatives, Guangdong Province has established 3,352.7 hectares of new mangroves and restored 2,354.46 hectares (data source: Guangdong Provincial Government). The coexistence of natural mangroves, restored mangroves, and adjacent tidal flats under different urbanization levels provided an opportunity to examine variations in carbon stocks and burial rates across an urbanization gradient.

2.2 Field sampling

Field sampling was conducted during summer across natural mangroves, restored mangroves, and adjacent tidal flats in Zhanjiang, Shantou, and Huizhou. The number of plots in each city was adjusted according to habitat area and field accessibility to ensure representative coverage of each habitat type along the urbanization gradient. Specifically, six sites were established in the natural mangroves of both Huizhou and Zhanjiang, whereas eight, eight, and six sites were established in the restored mangroves of Huizhou, Shantou, and Zhanjiang, respectively. Notably, no natural mangroves were identified in Shantou. Within each 10 m × 10 m plot, three parallel soil samples were collected for analyses of $\delta^{13}C$, $\delta^{15}N$, soil bulk density (SBD), soil organic carbon (SOC), total nitrogen (TN), total phosphorus (TP), and soil salinity. Leaf samples were also collected from each plot according to the local mangrove community composition.

During low tide, three representative 1-meter soil cores were collected from each plot using a soil corer with a diameter of 2.5 cm. Each core was sectioned in the field into eight layers: 0–5 cm, 5–10 cm, 10–20 cm, 20–30 cm, 30–45 cm, 45–60 cm, 60–80 cm, and 80–100 cm. To minimize errors due to sediment compaction, the actual penetration depth and core length were measured and recorded for each core, and a correction factor was applied following (Morton and White, 1997). Each soil sample was labeled and stored in a −20 °C freezer in the laboratory prior to further analysis. In addition, following the Technical Specification for Marine Environmental Monitoring Part 6: Coastal Biological Monitoring (HJ442.6-2020), phytoplankton samples were collected from nearby coastal waters. Five parallel 500 mL samples were obtained and stored in dark conditions to avoid light exposure. All samples were labeled and refrigerated prior to laboratory processing and analysis.

Due to the high cost of ^{210}Pb sediment dating, only one plot per mangrove type was selected in each city to measure sediment accumulation rates. It was assumed that mangroves of the same type under similar levels of urbanization had comparable sedimentation rates. Sediment accumulation rates for tidal flats were not assessed in this study. During low tide, three 1-meter soil cores were collected from each selected plot using stainless steel corers. Each core was sectioned at 2 cm intervals from 0 to 30 cm and at 10 cm intervals from 30 to 100 cm, resulting in a total of 22 layers (Huang et al., 2025b).

https://doi.org/10.5194/egusphere-2026-2512
Preprint. Discussion started: 13 May 2026

2.3 Lab analysis

2.3.1 Soil Parameter Measurements

Soil samples were oven-dried at 60 °C to a constant weight. After removing visible plant residues and shell fragments, the samples were ground and passed through a 0.2 mm sieve for the determination of TN, TP, salinity, and organic carbon. For salinity measurement, 50.0 g of air-dried soil was placed in a 500 mL dry Erlenmeyer flask, and 250 mL of deionized water was added. The flask was sealed and shaken at 220 rpm for 5 minutes. Salinity was then measured using a YSI ProPlus multi-parameter probe (YSI Inc., Ohio, USA). TP was determined after H_2SO_4–$HClO_4$ digestion and analyzed using a UV-1900i spectrophotometer (Shimadzu, Hong Kong). The detection limit was 9.0 mg kg-1 for a 0.25 g sample. TN was measured following Kjeldahl digestion and analyzed using an AA3 continuous flow analyzer, with a detection limit of 48 mg kg-1 for a 1 g sample. Inorganic carbon was removed using HCl solution, and organic carbon content was determined using a Vario EL III elemental analyzer (Elementar, Germany). SBD was calculated as the ratio of the oven-dried soil mass to the corresponding soil volume. SOC stock was calculated by multiplying the SBD, carbon content, and the corrected soil core depth.

2.3.2 ^{210}Pb Sediment Dating

^{210}Pb is a naturally occurring radionuclide in the ^{238}U decay series, with a half-life of 22.2 years, and is widely used to determine sediment chronology over timescales of up to approximately 150 years (Huang et al., 2025 ; Sasmito et al., 2020a). In this study, the constant rate of supply (CRS) model of ^{210}Pb dating was applied to estimate sediment accumulation rates (mm yr^{-1}). The analytical procedures followed the national standard Method for Gamma Spectrometric Determination of Radionuclides in Marine Sediments (GB/T 30738–2014), and measurements were performed using a high-purity germanium (HPGe) gamma spectrometer manufactured by Canberra (USA). Sample preparation and analysis were conducted by the technical team at the South China Sea Ecology Center, Ministry of Natural Resources. The primary radionuclides measured were ^{210}Pb, ^{226}Ra, and ^{137}Cs. The soil organic carbon burial rate was calculated by multiplying carbon density by the sediment accumulation rate (Huang et al., 2025b; Kauffman & Donato, 2012).

2.3.3 Stable Isotope Analysis

Soil samples were oven-dried, while plant samples were freeze-dried. All samples were ground and passed through a 0.2 mm sieve to ensure homogeneity. The samples were combusted at high temperature in a DELTA V Advantage isotope ratio mass spectrometer to produce CO_2 and N_2 gases. The instrument measured the $^{13}C/^{12}C$ ratio in CO_2 and the $^{15}N/^{14}N$ ratio in N_2. These values were compared against international reference standards to calculate $\delta^{13}C$ and $\delta^{15}N$ values. The isotopic ratios were calculated using the following equation (Eq. 1):

$$\delta = \left(\left(R_{sample}/R_{standard}\right) - 1\right) \times 1000 \quad (1)$$

https://doi.org/10.5194/egusphere-2026-2512
Preprint. Discussion started: 13 May 2026

Where δ is isotopic ratios (‰). *R*sample is the ratio of heavy to light isotopes ($^{13}C/^{12}C$ or $^{15}N/^{14}N$) in the sample, and *R*standard is the corresponding ratio in the international reference material. Vienna-Pee Dee Belemnite (VPDB) was used as the standard for $\delta^{13}C$, and atmospheric nitrogen (Atm-N_2) was used as the standard for $\delta^{15}N$. The analytical precision for $\delta^{13}C$ and $\delta^{15}N$ measurements was better than ±0.1‰ and ±0.2‰, respectively.

2.4 Data analysis

Prior to data analysis, the dataset was tested for normality and homogeneity of variances using the Shapiro-Wilk and Levene's tests, respectively. Data that did not meet these assumptions were subjected to rank-based inverse normal transformation to satisfy the requirements for parametric statistical analyses (Huang et al., 2024; Huang et al., 2025a). For datasets that still failed normality and homogeneity tests after transformation, non-parametric Kruskal-Wallis tests were applied (Zhang et al., 2022). All statistical analyses were performed using R version 4.4.3 (R Core Team, 2025).

Linear mixed-effects models were used to assess differences in total nitrogen, salinity, total phosphorus, bulk density, organic carbon content, organic carbon stock, organic carbon burial rate, and organic carbon turnover rate in soils from natural mangroves, restored mangroves, and tidal flats across varying levels of urbanization. Results were presented as mean ± standard deviation (mean ± SD), with significance set at $p < 0.05$.

This study employed dual-tracer stable isotope analysis ($\delta^{13}C$ and $\delta^{15}N$) and used the Bayesian mixing model MixSIAR on the R platform to estimate the contributions of different organic carbon sources in 0–100 cm sediment layers across various ecosystems under different urbanization backgrounds (Zhang et al., 2024). During model construction, mangrove leaf tissue and marine phytoplankton were selected as potential organic carbon end-members, with their $\delta^{13}C$ and $\delta^{15}N$ isotope values used as prior input variables. The model outputs provided the relative contributions of mangrove-derived and marine-derived organic carbon in sediments from natural mangroves, restored mangroves, and tidal flats.

Additionally, linear regression analyses were performed between the log10-transformed organic carbon content and $\delta^{13}C$ values for each 0–100 cm soil core sample. The slope of the regression function, denoted as β, was used as an indicator to assess SOC turnover rates (Huang et al., 2025b; Zhang et al., 2022). A higher β value indicated a lower SOC turnover rate and greater soil organic carbon stability (Acton et al., 2013; Xia et al., 2021; Zhao et al., 2019).

https://doi.org/10.5194/egusphere-2026-2512
Preprint. Discussion started: 13 May 2026

3 Results

3.1 Variations in soil physicochemical properties along an urbanization gradient

TN, TP, SBD, salinity and SOC contents showed significant variations along the urbanization gradient ($p < 0.05$), with distinct patterns observed among ecosystems. Specifically, in natural mangroves, salinity and bulk density differed significantly with urbanization level ($p < 0.05$), whereas TN, TP, and SOC contents did not vary significantly across the gradient (Table 1; Fig. 2a). Although SOC content in highly urbanized natural mangroves was higher than that in low-urbanization sites, it declined sharply with increasing soil depth (Fig. 3). In restored mangroves, TN, TP, SBD, and SOC contents varied significantly across high, moderate, and low urbanization levels ($p < 0.05$), while salinity showed a decreasing trend. SOC contents in moderately and low-urbanized restored mangroves were comparable. In tidal flats, urbanization significantly affected TN and SOC ($p < 0.05$), with the lowest SOC content observed under high urbanization conditions (Table 1; Fig. 3).

Table 1. Soil physicochemical properties of natural mangroves, restored mangroves, and tidal flats under different urbanization levels. Different letters indicated significant differences within the same mangrove type across varying urbanization levels ($p < 0.05$).

Types	Total nitrogen ($g\ kg^{-1}$)	Salinity ($g\ kg^{-1}$)	Total phosphorous ($g\ kg^{-1}$)	Soil bulk density ($g\ cm^{-3}$)
High-urbanization natural mangroves	2.54 ± 1.19 a	52.21 ± 13.54 b	0.56 ± 0.40 a	0.57 ± 0.22 a
Low-urbanization natural mangroves	2.56 ± 1.47 a	17.10 ± 5.56 a	0.39 ± 0.23 a	0.93 ± 0.33 b
High-urbanization restored mangroves	0.56 ± 0.37 a	17.94 ± 8.14 a	0.38 ± 0.14 ab	0.97 ± 0.16 b
Moderate -urbanization restored mangroves	1.40 ± 0.73 b	13.79 ± 10.09 a	0.49 ± 0.27 b	0.77 ± 0.24 a
Low-urbanization restored mangroves	1.48 ± 1.07 b	11.36 ± 4.04 a	0.28 ± 0.11 a	1.04 ± 0.32 b
High-urbanization tidal flats	0.33 ± 0.16 a	14.40 ± 4.83 a	0.26 ± 0.11 a	1.15 ± 0.11 a
Moderate -urbanization tidal flats	1.24 ± 1.05 b	12.16 ± 4.63 a	0.29 ± 0.20 a	0.93 ± 0.25 a
Low-urbanization tidal flats	1.37 ± 0.95 b	9.60 ± 3.99 a	0.42± 0.23 a	1.07 ± 0.29 a

https://doi.org/10.5194/egusphere-2026-2512
Preprint. Discussion started: 13 May 2026

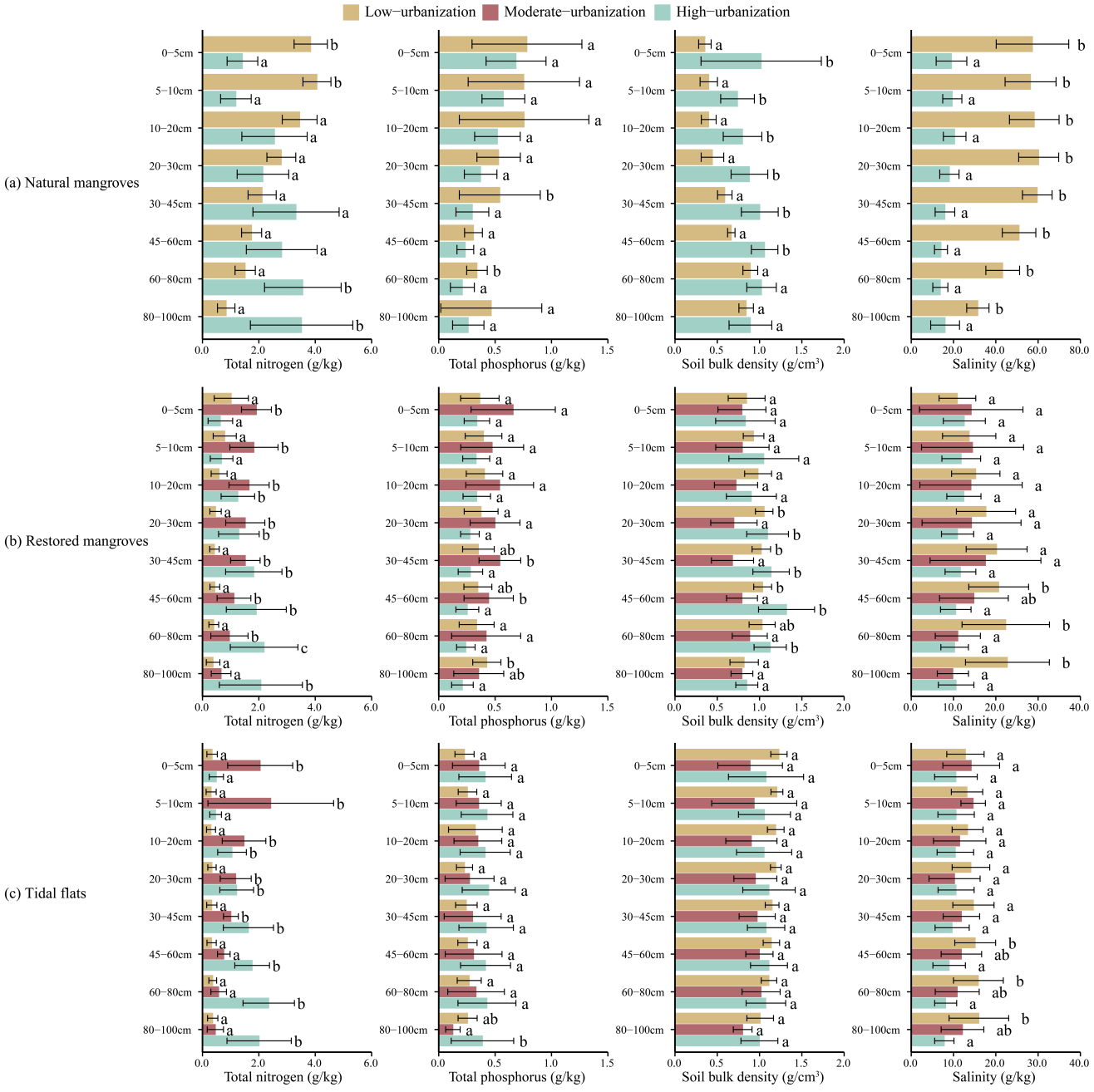

Figure 2. Values of total nitrogen, total phosphorus, soil bulk density and salinity, and in the 0-100 cm soil layer of natural mangroves, restored mangroves, and tidal flats under different levels of urbanization. Different letters indicated significant differences among urbanization levels ($p < 0.05$).

https://doi.org/10.5194/egusphere-2026-2512
Preprint. Discussion started: 13 May 2026

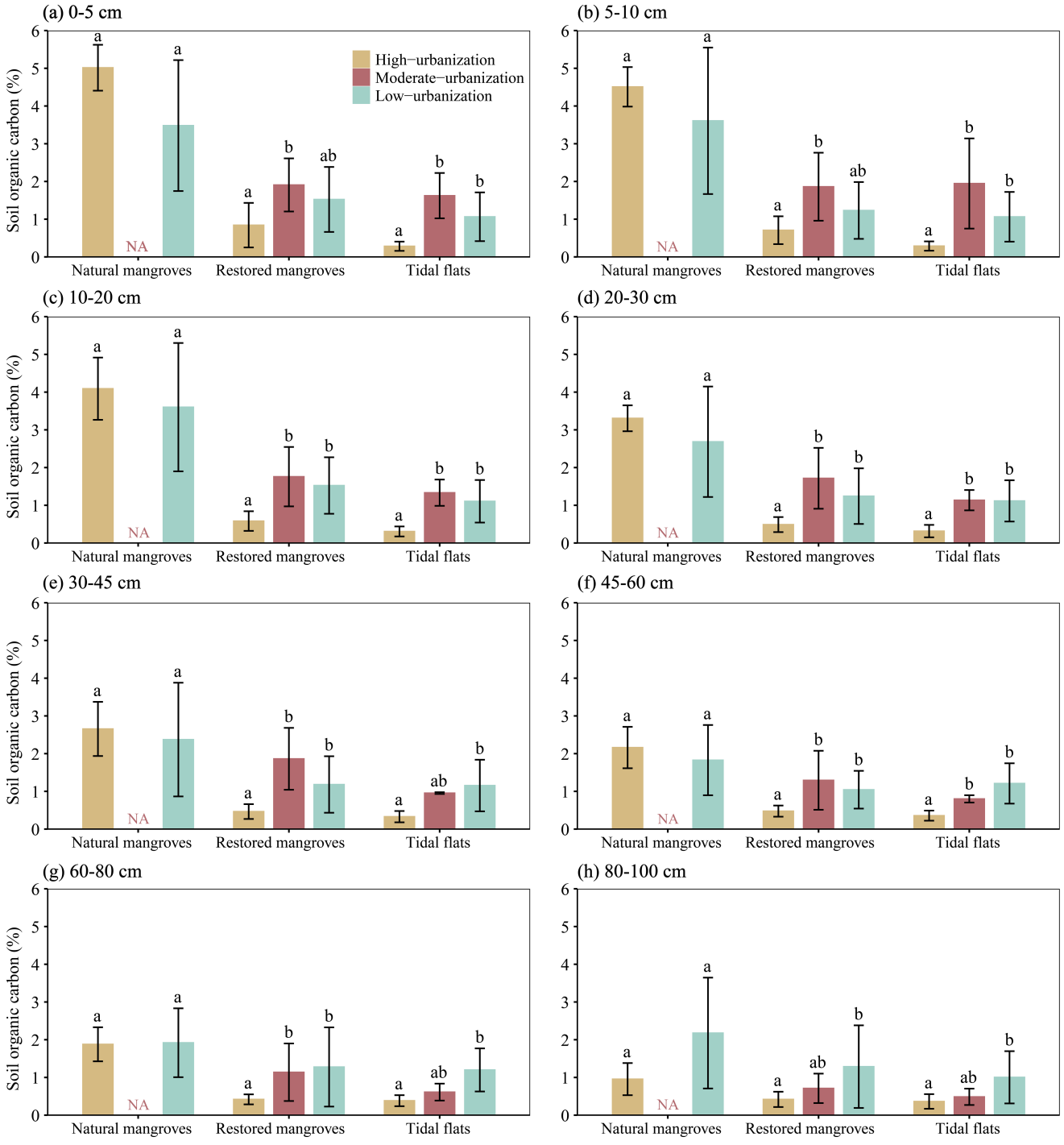

Figure 3. Vertical distribution of soil organic carbon in natural mangroves, restored mangroves, and tidal flats. Different letters indicated significant differences in soil organic carbon among urbanization levels within the same ecosystem type ($p < 0.05$).

https://doi.org/10.5194/egusphere-2026-2512
Preprint. Discussion started: 13 May 2026

3.2 Impacts of urbanization on SOC accumulation and burial

Consistent with H1, carbon accumulation declined with increasing urbanization, with the steepest reductions observed in highly urbanized natural and restored mangroves (Fig. 4). In low-urbanization areas, natural mangroves exhibited the highest SOC burial rate (426.44 ± 128.36 g C m^{-2} yr^{-1}), whereas restored mangroves peaked under moderate urbanization (267.19 ± 104.68 g C m^{-2} yr^{-1}). In both ecosystems, SOC burial rates were lowest in highly urbanized areas (Table 2). SOC stocks followed a similar trend, reaching minimum values in highly urbanized natural and restored mangroves as well as in tidal flats. Conversely, under moderate urbanization, SOC stocks in restored mangroves and tidal flats were comparable to those in low-urbanization areas ($p > 0.05$; Table 2).

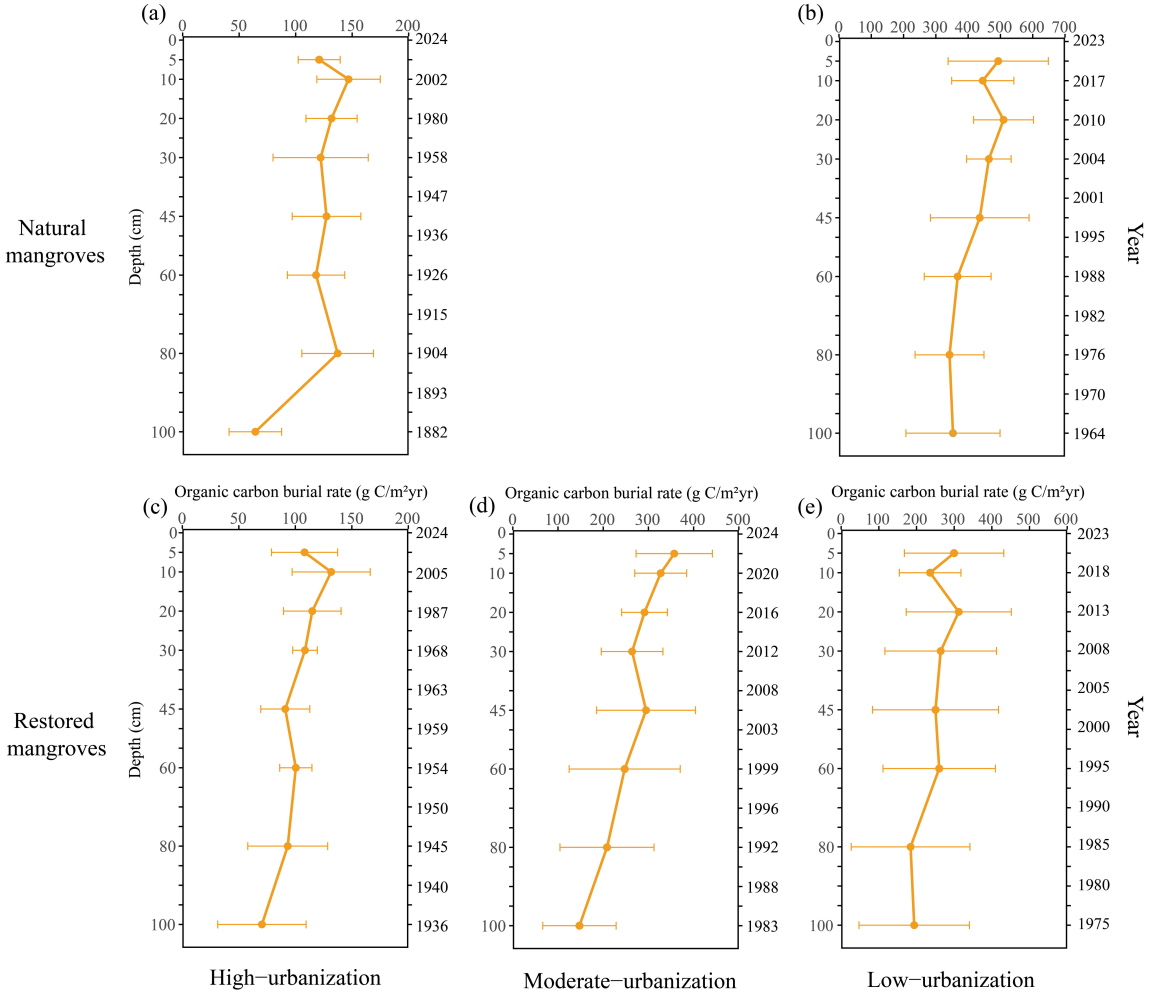

Figure 4. Vertical distribution of soil organic carbon burial rates and sediment ages in natural and restored mangroves under different levels of urbanization. Note: The x-axis titles in panels (a) and (b) were consistent with that in panel (c).

https://doi.org/10.5194/egusphere-2026-2512
Preprint. Discussion started: 13 May 2026

Table 2. Soil sedimentation rate, SOC burial rate, SOC stock, and SOC content across different ecosystem types. Different letters indicate significant differences among urbanization levels within the same mangrove type ($p < 0.05$).

Types	Sedimentation rate ($mm\ yr^{-1}$)	SOC burial rate ($g\ C\ m^{-2}\ yr^{-1}$)	SOC stocks ($Mg\ C\ ha^{-1}$)	SOC content (%)
High-urbanization natural mangroves	6.90	121.05 ± 35.28 a	168.07 ± 32.24 a	3.07 ± 1.43 a
Low-urbanization natural mangroves	16.36	426.44± 128.36 b	203.11 ±59.62 a	2.73 ± 1.61 a
High-urbanization restored mangroves	13.56	102.44 ± 31.47 a	56.02 ± 19.05 a	0.55 ± 0.32 a
Moderate-urbanization restored mangroves	24.87	267.19 ± 104.68 b	110.07 ± 23.08 b	1.53 ± 0.83 b
Low-urbanization restored mangroves	19.92	248.91 ± 142.90 b	122.22 ± 59.98 b	1.28 ± 0.82 b
High-urbanization tidal flats	NA	NA	42.65 ± 13.55 a	0.33 ± 0.14 a
Moderate -urbanization tidal flats	NA	NA	96.43 ± 5.61 b	1.11 ± 0.64 b
Low-urbanization tidal flats	NA	NA	113.73 ± 40.22 b	1.12 ± 0.60 b

Sedimentation rates also decreased along an urbanization gradient, with natural and restored mangroves in highly urbanized regions exhibiting the lowest rates of 6.90 mm yr^{-1} and 13.56 mm yr^{-1}, respectively (Table 2). Analyses of ^{210}Pb and ^{226}Ra indicated relatively older sediments, with depositional ages of 142 years for natural mangroves and 88 years for restored mangroves (Appendix A Fig. A1). Notably, a pronounced disturbance signal was detected at approximately 30 cm depth, corresponding to the period between 1958 and 1968.

3.3 Variations in the source contributions of SOC across ecosystems under urbanization stress

Consistent with H2, the sources of SOC in restored mangroves and tidal flats varied significantly along an urbanization gradient, whereas soils in natural mangroves remained dominated by mangrove-derived carbon (Fig. 5). Specifically, although the relative contribution of phytoplankton-derived carbon in natural mangroves increased by 18.82% from low to high urbanization levels, mangrove-derived carbon still accounted for the majority of SOC (Fig. 5a and b). In contrast, restored mangroves and tidal flats exhibited a pronounced shift in organic carbon composition—from mangrove-derived to phytoplankton-derived sources—with the latter becoming dominant under high urbanization. From low to high urbanization levels, mangrove-derived carbon inputs decreased by 49.63% and 57.26% in restored mangroves and tidal flats, respectively, while phytoplankton-derived carbon contributed more than 60% of the total SOC inputs in both ecosystems at highly urbanized sites (Fig. 5).

https://doi.org/10.5194/egusphere-2026-2512
Preprint. Discussion started: 13 May 2026

Figure 5. Vertical distribution of the relative contributions of soil organic carbon sources in the 0–100 cm soil layer of natural mangroves, restored mangroves, and tidal flats under different levels of urbanization.

Notably, the vertical profiles of SOC sources showed a similar trend. In highly and moderately urbanized areas, the relative contribution of phytoplankton-derived carbon increased with depth, indicating sustained external inputs and long-term burial. In contrast, soils in low-urbanization regions were consistently dominated by mangrove-derived carbon across all depths, suggesting that these ecosystems maintained ecological stability under minimal urban disturbance (Fig. 5; Appendix A Table A2).

https://doi.org/10.5194/egusphere-2026-2512
Preprint. Discussion started: 13 May 2026

3.4 Urbanization-driven shifts in soil carbon pool stability across ecosystems

Consistent with H3, the β values representing SOC turnover rates in natural mangroves, restored mangroves, and tidal flats decreased along the low-to-high urbanization gradient (Fig. 6). Among the three ecosystems, the highly urbanized areas exhibited the lowest β values, indicating the fastest SOC turnover and consequently the lowest carbon pool stability. In contrast, across all levels of urbanization, tidal flats had generally higher β values than mangroves, suggesting that SOC in tidal flats was relatively more stable. Overall, increasing urbanization accelerated SOC turnover and reduced soil carbon stability in coastal ecosystems, with mangrove habitats showing more pronounced instability.

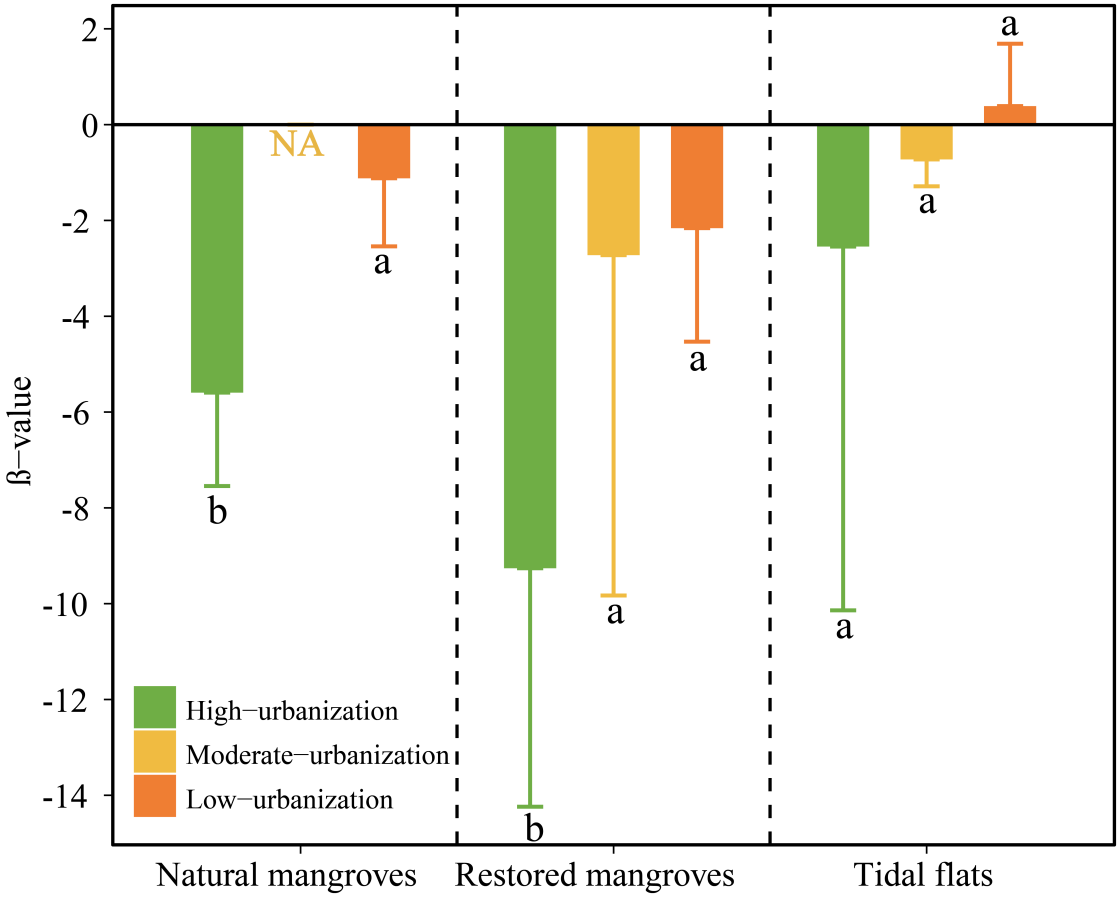

Figure 6. Soil β-values in natural mangroves, restored mangroves, and tidal flats under different levels of urbanization. Different letters indicated significant differences in β-values among urbanization levels within the same ecosystem type ($p < 0.05$).

4 Discussion

Our results illustrate that urbanization reduces soil-carbon stocks and burial and that this decline is amplified by two coordinated responses: source composition shifts away from mangrove-derived inputs and the stability of the soil-carbon pool decreases. The novelty is to treat these outcomes not as parallel symptoms but as a single, integrated pathway that links "how

https://doi.org/10.5194/egusphere-2026-2512
Preprint. Discussion started: 13 May 2026

much is stored," "who supplies it," and "how long it persists." Our data indicate that this three-part linkage is strongest in restored mangroves and adjacent tidal flats, where geomorphic memory and belowground integrity are weaker, whereas natural mangroves in low-urbanization settings function as regional carbon anchors that combine higher stocks, mangrove-dominated inputs, and slower turnover rate. Framing blue carbon through this integrated triad advances urban-coast studies that have focused mainly on quantity and clarifies why managing sources and stability is as critical as safeguarding stocks and burial.

Our results suggest that urbanization consistently depresses carbon burial and stocks, yet the response is not strictly linear. Natural mangroves in low urbanization settings, with mature belowground structure and long geomorphic memory, retain the highest sequestration, whereas restored mangroves and tidal flats on younger or reworked substrates show steeper declines as pressure intensifies. Mechanistically, this observed quantity pattern reflects the physical side of a single pathway from carbon production to preservation. Urban development reduces tidal hydrological and sediment connectivity, limits vertical accretion, and increases oxygen exposure of legacy layers (Lovelock et al., 2017; Sasmito, et al., 2020b; Willemsen et al., 2016), and these effects intensify where aquaculture, land reclamation, and urban infrastructure disrupt sediment regimes and promote remineralization (Wei et al., 2024). In parallel, salinity shifts and nutrient imbalance constrain stomatal conductance and photosynthetic efficiency, lowering mangrove productivity and the detrital supply that supports burial (Huang et al., 2025a). By contrast, low urbanization natural mangroves maintain tidal connectivity, sustained sediment delivery, and long-term nutrient cycling that favor persistent anoxia and longer residence times (Huang et al., 2025a; Marchio et al., 2016). When connectivity and accretion remain above habitat specific limits, losses are buffered (Marchio et al., 2016; Saintilan et al., 2020). Once those limits are crossed, previously buried horizons return to active cycling and carbon stocks decline rapidly, which produces the observed nonlinearity.

Our data show that urbanization shifts soil carbon sources in a habitat-dependent way. As urban intensity increases, natural mangrove soils remain mangrove-dominated, whereas restored mangroves and tidal flats shift strongly toward planktonic and algal inputs. Depth profiles at more urbanized sites indicate that these external, labile inputs are persistently buried through time, whereas low-urbanization soils keep a mangrove signature across depth. Our results point to two drivers of this shift under urban pressure. First, our restored stands are early in succession; underdeveloped root systems and physiological stress associated with salinity and nutrient imbalance depress productivity and litter inputs, so mangrove detrital supply declines (Dung et al., 2016; Huang et al., 2025a; Ram et al., 2024). Second, urban practices and coastal setting increase the delivery and retention of marine organic matter through channel excavation and deepening, intensified water exchange, and re-exposure of plankton-rich sediments, with tidal flats amplifying this effect through frequent flushing (Barroso et al., 2022; Breitburg et al., 2018; Grilo et al., 2013; Huang et al., 2025b). Together, these results confirm H2 and identify source composition as the operative bridge linking urban-driven geomorphic and physiological change to reduced carbon durability.

https://doi.org/10.5194/egusphere-2026-2512
Preprint. Discussion started: 13 May 2026

Our results indicate that soil carbon stability declines along the urbanization gradient, with the steepest losses in mangrove habitats. This pattern follows the source shift documented in H2: under strong urban pressure, inputs move from structurally complex mangrove detritus to more labile marine material, which accumulates easily decomposable compounds and accelerates carbon loss (Bouillon et al., 2008; Zhang et al., 2024). In parallel, land reclamation and coastal engineering reduce sediment deposition and tidal connectivity, weakening the biophysical feedbacks that sustain anoxia and mineral protection and thereby increasing SOC degradability as urbanization intensifies (Barroso et al., 2022; Deng et al., 2024; Kirwan et al., 2016). In our most urbanized sites, precise 210Pb dating was difficult, consistent with stronger bioturbation and erosion and deposition disturbance that remix and expose younger material (Huang et al., 2025b). Habitat fragmentation further erodes resilience and long-term stability (Turschwell et al., 2020). Accordingly, we treat stability as an operational metric rather than an inferred property. A composite stability index that couples turnover rates with chemical or thermal proxies can be tracked alongside stocks and sources, used to set early-warning thresholds, and applied to guide stability-first restoration and protection in urbanized coastal systems.

Taken together, along the urbanization gradient, carbon stocks, sources, and stability operate as coupled state variables with predictable, decision-relevant dynamics. This coupling yields two transferable system states: carbon anchors in low-urbanization natural mangroves, where mangrove-dominated inputs co-occur with slow turnover, and instability fronts in restored stands and tidal flats, where urban pressure pushes systems past habitat-specific thresholds, sources shift toward labile marine material, and residence times shorten. Within this frame, changes in sources and stability act as leading indicators that foreshadow quantity losses and help explain the nonlinear response in H1, so H2 and H3 move from description to diagnosis. Management follows directly by prioritizing the protection of anchor sites in low-urbanization landscapes and by implementing stability-first restoration that tracks explicit thresholds for connectivity, accretion, sources, and stability to trigger timely action.

5 Conclusions

Our study shows that urbanization reorganizes blue carbon function in mangrove–tidal-flat mosaics, driving coupled declines in soil carbon stocks and burial, a shift away from mangrove detritus, and faster turnover that lowers stability. We present a triad framework that treats carbon stocks, sources, and stability as coupled state variables along the urbanization gradient and reveal two reproducible states: carbon anchors in low-urbanization natural mangroves and instability fronts in restored stands and tidal flats. This frame explains heterogeneous urban responses and provides leading indicators, as carbon source and stability shift often precede stock loss. It also yields a compact diagnostic to prioritize anchor protection and stability-first restoration where urban pressure is highest. Future work should scale from sites to city regions, integrate urban growth and coastal-risk scenarios, and set policy thresholds for carbon accretion, sources, and stability.

https://doi.org/10.5194/egusphere-2026-2512
Preprint. Discussion started: 13 May 2026

Appendix A

Table A1. Quantitative comparison of socioeconomic indicators used to classify the urbanization gradient, with Huizhou, Shantou, and Zhanjiang representing high, moderate, and low urbanization levels, respectively.

City	Year	Urban population proportion (%)	Non-agricultural population proportion (%)	Per capita disposable income of urban residents (CNY)	Built-up area (km^2)
Huizhou	2023	73.30	90.51	52621	429.59
Shantou	2023	71.15	86.28	38070	279.42
Zhanjiang	2023	48.07	72.50	37498	243.53
Huizhou	2022	72.91	89.75	37099	413.93
Shantou	2022	70.75	85.45	35989	279.61
Zhanjiang	2022	47.31	70.70	37099	241.60
Huizhou	2021	72.90	89.21	49243	409.53
Shantou	2021	70.74	85.24	35601	247.05
Zhanjiang	2021	46.46	70.30	35989	241.63
Huizhou	2020	72.80	88.92	45475	391.61
Shantou	2020	70.70	84.90	32922	291.81
Zhanjiang	2020	45.46	69.70	32926	253.92
Huizhou	2019	72.12	88.28	42999	375.78
Shantou	2019	70.44	75.88	31416	291.81
Zhanjiang	2019	42.88	68.40	31241	241.05
Huizhou	2018	70.76	87.90	39574	365.50
Shantou	2018	70.41	74.29	29077	281.65
Zhanjiang	2018	41.33	67.60	29046	240.67
Huizhou	2017	69.55	86.99	36608	355.70
Shantou	2017	70.39	74.01	27175	277.22
Zhanjiang	2017	39.72	62.10	27119	239.52
Huizhou	2016	69.05	86.15	33213	342.74
Shantou	2016	70.30	73.79	25121	257.66
Zhanjiang	2016	39.22	59.20	24887	245.24
Huizhou	2015	68.15	85.26	30057	279.12
Shantou	2015	70.22	72.97	23260	253.60
Zhanjiang	2015	38.67	56.30	23129	242.84
Huizhou	2014	NA	84.42	27300	309.60
Shantou	2014	NA	72.79	21446	250.42
Zhanjiang	2014	NA	53.00	21317	240.71

https://doi.org/10.5194/egusphere-2026-2512
Preprint. Discussion started: 13 May 2026

Huizhou	2013	NA	83.26	24293	302.80
Shantou	2013	NA	72.79	22207	247.39
Zhanjiang	2013	NA	50.10	22371	210.07

Table A2. Relative contributions of sediment organic carbon (OC) originating from phytoplankton and mangrove sources in natural mangroves, restored mangroves, and tidal flats along an urbanization gradient.

Types	Depth (cm)	Mangrove OC (%)	Phytoplankton OC (%)
High-urbanization natural mangroves	0-5	77.40	22.60
High-urbanization natural mangroves	5-10	77.90	22.10
High-urbanization natural mangroves	10-20	75.90	24.10
High-urbanization natural mangroves	20-30	70.90	29.10
High-urbanization natural mangroves	30-45	69.40	30.60
High-urbanization natural mangroves	45-60	68.90	31.10
High-urbanization natural mangroves	60-80	68.70	31.30
High-urbanization natural mangroves	80-100	56.30	43.70
High-urbanization restored mangroves	0-5	43.70	56.30
High-urbanization restored mangroves	5-10	44.40	55.60
High-urbanization restored mangroves	10-20	41.60	58.40
High-urbanization restored mangroves	20-30	35.70	64.30
High-urbanization restored mangroves	30-45	34.00	66.00
High-urbanization restored mangroves	45-60	33.50	66.50
High-urbanization restored mangroves	60-80	33.40	66.60
High-urbanization restored mangroves	80-100	23.00	77.00
High-urbanization tidal flats	0-5	32.10	67.90
High-urbanization tidal flats	5-10	32.80	67.80
High-urbanization tidal flats	10-20	30.30	69.70
High-urbanization tidal flats	20-30	25.30	74.70
High-urbanization tidal flats	30-45	24.00	76.00
High-urbanization tidal flats	45-60	23.60	76.40
High-urbanization tidal flats	60-80	23.50	76.50
High-urbanization tidal flats	80-100	15.60	84.40
Moderate -urbanization restored mangroves	0-5	68.50	31.50
Moderate -urbanization restored mangroves	5-10	68.80	31.20
Moderate -urbanization restored mangroves	10-20	67.60	32.40
Moderate -urbanization restored mangroves	20-30	66.40	33.60
Moderate -urbanization restored mangroves	30-45	64.20	35.80
Moderate -urbanization restored mangroves	45-60	55.60	44.40

https://doi.org/10.5194/egusphere-2026-2512
Preprint. Discussion started: 13 May 2026

Moderate -urbanization restored mangroves	60-80	49.00	51.00
Moderate -urbanization restored mangroves	80-100	51.10	48.90
Moderate -urbanization tidal flats	0-5	67.00	33.00
Moderate -urbanization tidal flats	5-10	67.40	32.60
Moderate -urbanization tidal flats	10-20	66.10	33.90
Moderate -urbanization tidal flats	20-30	64.80	35.20
Moderate -urbanization tidal flats	30-45	62.70	37.30
Moderate -urbanization tidal flats	45-60	54.00	46.00
Moderate -urbanization tidal flats	60-80	47.40	52.60
Moderate -urbanization tidal flats	80-100	49.50	50.50
Low-urbanization natural mangroves	0-5	86.90	13.10
Low-urbanization natural mangroves	5-10	88.90	11.10
Low-urbanization natural mangroves	10-20	89.40	10.60
Low-urbanization natural mangroves	20-30	89.10	10.90
Low-urbanization natural mangroves	30-45	89.80	10.20
Low-urbanization natural mangroves	45-60	90.10	9.90
Low-urbanization natural mangroves	60-80	90.60	9.40
Low-urbanization natural mangroves	80-100	91.10	8.90
Low-urbanization restored mangroves	0-5	82.60	17.40
Low-urbanization restored mangroves	5-10	85.10	14.90
Low-urbanization restored mangroves	10-20	85.10	14.90
Low-urbanization restored mangroves	20-30	85.40	14.60
Low-urbanization restored mangroves	30-45	86.30	13.70
Low-urbanization restored mangroves	45-60	86.60	13.40
Low-urbanization restored mangroves	60-80	87.30	12.70
Low-urbanization restored mangroves	80-100	87.90	12.10
Low-urbanization tidal flats	0-5	79.60	20.40
Low-urbanization tidal flats	5-10	82.50	17.50
Low-urbanization tidal flats	10-20	83.30	16.70
Low-urbanization tidal flats	20-30	82.80	17.20
Low-urbanization tidal flats	30-45	83.90	16.10
Low-urbanization tidal flats	45-60	84.30	15.70
Low-urbanization tidal flats	60-80	85.10	14.90
Low-urbanization tidal flats	80-100	85.80	14.20

https://doi.org/10.5194/egusphere-2026-2512
Preprint. Discussion started: 13 May 2026

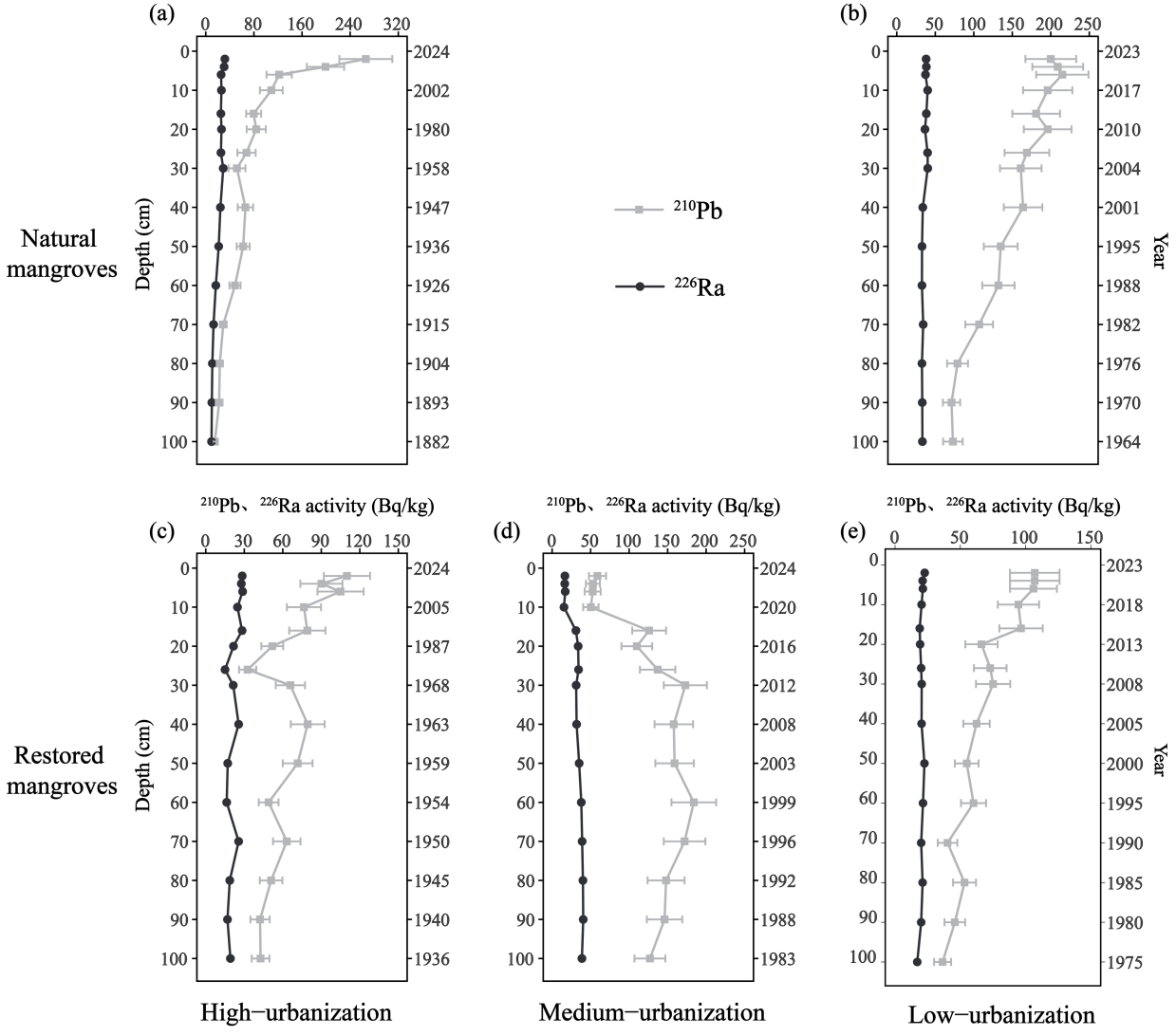

Figure A1. Vertical profiles of soil age and ^{210}Pb and ^{226}Ra activities in natural and restored mangroves under varying urbanization levels.

Data availability

The data supporting this study are publicly available via GitHub at https://github.com/lizhe-hmd/Impacts-of-urbanization-on-blue-carbon-ecosystems.git.

https://doi.org/10.5194/egusphere-2026-2512
Preprint. Discussion started: 13 May 2026

Author contributions

Minde Huang: Writing – original draft, Methodology, Investigation, Data curation. Fen Guo: Writing – review & editing, Validation, Supervision, Funding acquisition, Data curation, Conceptualization. Xueqin Gao: Writing – review & editing, Methodology, Investigation. Xiaoguang Ouyang: Writing – review & editing, Methodology, Data curation. Yuan Zhang: Writing – review & editing, Methodology.

Competing interests

The authors declare that they have no known competing financial interests or personal relationships that could have appeared to influence the work reported in this paper.

Disclaimer

Copernicus Publications adds a standard disclaimer: "Copernicus Publications remains neutral with regard to jurisdictional claims made in the text, published maps, institutional affiliations, or any other geographical representation in this paper. While Copernicus Publications makes every effort to include appropriate place names, the final responsibility lies with the authors. Views expressed in the text are those of the authors and do not necessarily reflect the views of the publisher."

Acknowledgements

We gratefully acknowledge the assistance of Huang Zixun, Zhang Yiming, Yang Zhenmin, Xing Wanli, Wu Junya, and Song Hua. AI tools were used to check for grammar and literature search.

Financial support

This work is supported by the National Key Research and Development Program of China (2024YFF0808802), the National Natural Science Foundation of China (52471276, 52388101, 52239005 and 52271280), and the Nansha Key Scientific and Technological Project, Guangdong Province (2023ZD012).

Review statement

The review statement will be added by Copernicus Publications listing the handling editor as well as all contributing referees according to their status anonymous or identified.

https://doi.org/10.5194/egusphere-2026-2512
Preprint. Discussion started: 13 May 2026

References

Acton, P., Fox, J., Campbell, E., Rowe, H., and Wilkinson, M.: Carbon isotopes for estimating soil decomposition and physical mixing in well-drained forest soils, JGR Biogeosciences, 118, 1532–1545, https://doi.org/10.1002/2013jg002400, 2013.

Ai, B., Ma, C., Zhao, J., and Zhang, R.: The impact of rapid urban expansion on coastal mangroves: A case study in guangdong province, China, Front. Earth Sci., 14, 37–49, https://doi.org/10.1007/s11707-019-0768-6, 2020.

Atwood, T. B., Connolly, R. M., Almahasheer, H., Carnell, P. E., Duarte, C. M., Ewers Lewis, C. J., Irigoien, X., Kelleway, J. J., Lavery, P. S., Macreadie, P. I., Serrano, O., Sanders, C. J., Santos, I., Steven, A. D. L., and Lovelock, C. E.: Global patterns in mangrove soil carbon stocks and losses, Nat. Clim. Change, 7, 523–528, https://doi.org/10.1038/nclimate3326, 2017.

Barroso, G. C., Abril, G., Machado, W., Abuchacra, R. C., Peixoto, R. B., Bernardes, M., Marques, G. S., Sanders, C. J., Oliveira, G. B., Oliveira Filho, S. R., Amora-Nogueira, L., and Marotta, H.: Linking eutrophication to carbon dioxide and methane emissions from exposed mangrove soils along an urban gradient, Science of The Total Environment, 850, 157988, https://doi.org/10.1016/j.scitotenv.2022.157988, 2022.

Bouillon, S., Borges, A. V., Castaneda-Moya, E., Diele, K., Dittmar, T., Duke, N. C., Kristensen, E., Lee, S. Y., Marchand, C., Middelburg, J. J., Rivera-Monroy, V. H., Smith, T. J., and Twilley, R. R.: Mangrove production and carbon sinks: A revision of global budget estimates, Glob. Biogeochem. Cycle, 22, GB2013, https://doi.org/10.1029/2007GB003052, 2008.

Branoff, B. L.: Quantifying the influence of urban land use on mangrove biology and ecology: A meta-analysis, Global Ecol Biogeogr, 26, 1339–1356, https://doi.org/10.1111/geb.12638, 2017.

Breitburg, D., Levin, L. A., Oschlies, A., Grégoire, M., Chavez, F. P., Conley, D. J., Garçon, V., Gilbert, D., Gutiérrez, D., Isensee, K., Jacinto, G. S., Limburg, K. E., Montes, I., Naqvi, S. W. A., Pitcher, G. C., Rabalais, N. N., Roman, M. R., Rose, K. A., Seibel, B. A., Telszewski, M., Yasuhara, M., and Zhang, J.: Declining oxygen in the global ocean and coastal waters, Science, 359, eaam7240, https://doi.org/10.1126/science.aam7240, 2018.

Chen, G., Gao, M., Pang, B., Chen, S., and Ye, Y.: Top-meter soil organic carbon stocks and sources in restored mangrove forests of different ages, Forest Ecol. Manag., 422, 87–94, https://doi.org/10.1016/j.foreco.2018.03.044, 2018.

Deng, P., Zhou, Q., Luo, J., Hu, X., and Yu, F.: Urbanization influences dissolved organic matter characteristics but microbes affect greenhouse gas concentrations in lakes, Science of The Total Environment, 912, 169191, https://doi.org/10.1016/j.scitotenv.2023.169191, 2024.

Dung, L. V., Tue, N. T., Nhuan, M. T., and Omori, K.: Carbon storage in a restored mangrove forest in Can Gio Mangrove Forest Park, Mekong Delta, Vietnam, For. Ecol. Manage., 380, 31–40, https://doi.org/10.1016/j.foreco.2016.08.032, 2016.

Fu, B., Fang, C., Xia, J., Pan, S., Zhou, L., Peng, Y., Yan, Y., Yang, Y., He, Y., Chen, S., Yang, H., and Wang, J.: Urbanization alters soil bacterial communities in southern China coastal cities, Ecotoxicology and Environmental Safety, 250, 114492, https://doi.org/10.1016/j.ecoenv.2022.114492, 2023.

Grilo, C. F., Neto, R. R., Vicente, M. A., De Castro, E. V. R., Figueira, R. C. L., and Carreira, R. S.: Evaluation of the influence of urbanization processes using mangrove and fecal markers in recent organic matter in a tropical tidal flat estuary, Appl. Geochem., 38, 82–91, https://doi.org/10.1016/j.apgeochem.2013.08.009, 2013.

Hamilton, S. E. and Friess, D. A.: Global carbon stocks and potential emissions due to mangrove deforestation from 2000 to 2012, Nat. Clim. Change, 8, 240-+, https://doi.org/10.1038/s41558-018-0090-4, 2018.

https://doi.org/10.5194/egusphere-2026-2512
Preprint. Discussion started: 13 May 2026

Hao, Q., Song, Z., Zhang, X., He, D., Guo, L., Van Zwieten, L., Yu, C., Wang, Y., Wang, W., Fang, Y., Fang, Y., Liu, C.-Q., and Wang, H.: Organic blue carbon sequestration in vegetated coastal wetlands: processes and influencing factors, Earth Sci. Rev., 255, 104853, https://doi.org/10.1016/j.earscirev.2024.104853, 2024.

Hong Tinh, P., Thi Hong Hanh, N., Van Thanh, V., Sy Tuan, M., Van Quang, P., Sharma, S., and MacKenzie, R. A.: A comparison of soil carbon stocks of intact and restored mangrove forests in Northern Vietnam, Forests, 11, 660, https://doi.org/10.3390/f11060660, 2020.

Huang, M., Guo, F., Ouyang, X., Gao, X., Zhu, Z., Zeng, X., and Zhang, Y.: Exploring soil carbon drivers across natural mangroves, restored mangroves, and tidal flats: implications for subtropical coastal carbon management, Catena, 252, 108875, https://doi.org/10.1016/j.catena.2025.108875, 2025a.

Huang, Z., Wang, Y., Guo, F., Ouyang, X., Zhu, Z., and Zhang, Y.: Mangrove soil carbon stocks varied significantly across community compositions and environmental gradients in the largest mangrove wetland reserve, China, Reg. Environ. Change, 24, 140, https://doi.org/10.1007/s10113-024-02307-3, 2024.

Huang, Z., Guo, F., Ouyang, X., Xiong, L., Zhu, Z., and Zhang, Y.: Differential carbon stocks and burial rates in natural versus planted mangrove forests under varied hydrogeomorphic conditions, CATENA, 254, 108981, https://doi.org/10.1016/j.catena.2025.108981, 2025b.

Jimenez, L. C. Z., Queiroz, H. M., Otero, X. L., Nóbrega, G. N., and Ferreira, T. O.: Soil organic matter responses to mangrove restoration: A replanting experience in northeast brazil, Int. J. Environ. Res. Public Health, 18, 8981, https://doi.org/10.3390/ijerph18178981, 2021.

Kang, L., Huamei, H., Ran, Y., Shengpeng, Z., Di, D., and Bo, P.: Carbon storage potential and influencing factors of mangrove plantation in Kaozhouyang, Guangdong Province, South China, Front. Mar. Sci., 11, https://doi.org/10.3389/fmars.2024.1439266, 2025.

Kauffman, J. B. and Donato, D. C.: Protocols for the measurement, monitoring and reporting of structure, biomass and carbon stocks in mangrove forests, Center for International Forestry Research (CIFOR), https://doi.org/10.17528/cifor/003749, 2012.

Kauffman, J. B., Bernardino, A. F., Ferreira, T. O., Bolton, N. W., Gomes, L. E. D. O., and Nobrega, G. N.: Shrimp ponds lead to massive loss of soil carbon and greenhouse gas emissions in northeastern Brazilian mangroves, Ecology and Evolution, 8, 5530–5540, https://doi.org/10.1002/ece3.4079, 2018.

Kauffman, J. B., Adame, M. F., Arifanti, V. B., Schile-Beers, L. M., Bernardino, A. F., Bhomia, R. K., Donato, D. C., Feller, I. C., Ferreira, T. O., Jesus Garcia, M. D. C., MacKenzie, R. A., Megonigal, J. P., Murdiyarso, D., Simpson, L., and Hernández Trejo, H.: Total ecosystem carbon stocks of mangroves across broad global environmental and physical gradients, Ecol. Monogr., 90, e01405, https://doi.org/10.1002/ecm.1405, 2020.

Kirwan, M. L., Temmerman, S., Skeehan, E. E., Guntenspergen, G. R., and Fagherazzi, S.: Overestimation of marsh vulnerability to sea level rise, Nat. Clim. Chang., 6, 253–260, https://doi.org/10.1038/NCLIMATE2909, 2016.

Lee, S. Y.: From blue to black: Anthropogenic forcing of carbon and nitrogen influx to mangrove-lined estuaries in the South China Sea, Marine Pollution Bulletin, 109, 682–690, https://doi.org/10.1016/j.marpolbul.2016.01.008, 2016.

Liao, H., Zhou, Y., Zhou, W., Wang, H., Liu, D., Wang, Y., and Cheng, H.: Spatial pattern and driving factors of carbon storage in mangroves along LeiZhou Peninsula, China, Ecological Indicators, 176, 113740, https://doi.org/10.1016/j.ecolind.2025.113740, 2025.

https://doi.org/10.5194/egusphere-2026-2512
Preprint. Discussion started: 13 May 2026

Lin, W., Wu, J., and Lin, H.: Contribution of unvegetated tidal flats to coastal carbon flux, Global Change Biology, 26, 3443–3454, https://doi.org/10.1111/gcb.15107, 2020.

Liu, T., Bao, K., Chen, M., Neupane, B., Gao, C., and Zaccone, C.: Human activity has increasingly affected recent carbon accumulation in Zhanjiang mangrove wetland, South China, iScience, 27, 109038, https://doi.org/10.1016/j.isci.2024.109038, 2024.

Lovelock, C. E. and Reef, R.: Variable impacts of climate change on blue carbon, One Earth, 3, 195–211, https://doi.org/10.1016/j.oneear.2020.07.010, 2020.

Lovelock, C. E., Fourqurean, J. W., and Morris, J. T.: Modeled CO2 emissions from coastal wetland transitions to other land uses: Tidal marshes, mangrove forests, and seagrass beds, Front. Mar. Sci., 4, 143, https://doi.org/10.3389/fmars.2017.00143, 2017.

Marchio, D., Savarese, M., Bovard, B., and Mitsch, W.: Carbon sequestration and sedimentation in mangrove swamps influenced by hydrogeomorphic conditions and urbanization in Southwest Florida, Forests, 7, 116, https://doi.org/10.3390/f7060116, 2016.

Morton, R. A. and White, W. A.: Characteristics of and corrections for core shortening in unconsolidated sediments, J. Coastal Res., 13, 761–769, 1997.

Ouyang, X. and Lee, S. Y.: Improved estimates on global carbon stock and carbon pools in tidal wetlands, Nat. Commun., 11, 317, https://doi.org/10.1038/s41467-019-14120-2, 2020.

R Core Team: R: A Language and Environment for Statistical Computing, 2025.

Ram, M., Sheaves, M., and Waltham, N. J.: Tracking the long-term vegetation and soil characteristics of restored mangroves: a case study from Guyana's coast, RESTORATION ECOLOGY, 32, https://doi.org/10.1111/rec.14170, 2024.

Saintilan, N., Khan, N. S., Ashe, E., Kelleway, J. J., Rogers, K., Woodroffe, C. D., and Horton, B. P.: Thresholds of mangrove survival under rapid sea level rise, Science, 368, 1118–1121, https://doi.org/10.1126/science.aba2656, 2020.

Sasmito, S. D., Sillanpää, M., Hayes, M. A., Bachri, S., Saragi-Sasmito, M. F., Sidik, F., Hanggara, B. B., Mofu, W. Y., Rumbiak, V. I., Hendri, Taberima, S., Suhaemi, Nugroho, J. D., Pattiasina, T. F., Widagti, N., Barakalla, Rahajoe, J. S., Hartantri, H., Nikijuluw, V., Jowey, R. N., Heatubun, C. D., Zu Ermgassen, P., Worthington, T. A., Howard, J., Lovelock, C. E., Friess, D. A., Hutley, L. B., and Murdiyarso, D.: Mangrove blue carbon stocks and dynamics are controlled by hydrogeomorphic settings and land-use change, Global Change Biol., 26, 3028–3039, https://doi.org/10.1111/gcb.15056, 2020a.

Sasmito, S. D., Kuzyakov, Y., Lubis, A. A., Murdiyarso, D., Hutley, L. B., Bachri, S., Friess, D. A., Martius, C., and Borchard, N.: Organic carbon burial and sources in soils of coastal mudflat and mangrove ecosystems, CATENA, 187, 104414, https://doi.org/10.1016/j.catena.2019.104414, 2020b.

Spivak, A. C., Sanderman, J., Bowen, J. L., Canuel, E. A., and Hopkinson, C. S.: Global-change controls on soil-carbon accumulation and loss in coastal vegetated ecosystems, Nat. Geosci., 12, 685–692, https://doi.org/10.1038/s41561-019-0435-2, 2019.

Sun, D., Huang, Y., Wang, Z., Tang, X., Ye, W., Cao, H., and Shen, H.: Soil microbial community structure, function and network along a mangrove forest restoration chronosequence, SCIENCE OF THE TOTAL ENVIRONMENT, 913, 169704, https://doi.org/10.1016/j.scitotenv.2023.169704, 2024.

https://doi.org/10.5194/egusphere-2026-2512
Preprint. Discussion started: 13 May 2026

Tang D., Xin C., Chen N., Liu X., and Zhang L.: Mangrove forest fragmentation and its ecological service value in Tongming Sea of Zhanjiang, Guangdong, China during 2000-2018, Chinese Journal of Applied Ecology, 34, 415–422, https://doi.org/10.13287/j.1001-9332.202302.022, 2023.

Turschwell, M. P., Tulloch, V. J. D., Sievers, M., Pearson, R. M., Andradi-Brown, D. A., Ahmadia, G. N., Connolly, R. M., Bryan-Brown, D., Lopez-Marcano, S., Adame, M. F., and Brown, C. J.: Multi-scale estimation of the effects of pressures and drivers on mangrove forest loss globally, Biol. Conserv., 247, 108637, https://doi.org/10.1016/j.biocon.2020.108637, 2020.

Wang, F., Liu, J., Qin, G., Zhang, J., Zhou, J., Wu, J., Zhang, L., Thapa, P., Sanders, C. J., Santos, I. R., Li, X., Lin, G., Weng, Q., Tang, J., Jiao, N., and Ren, H.: Coastal blue carbon in China as a nature-based solution toward carbon neutrality, The Innovation, 4, 100481, https://doi.org/10.1016/j.xinn.2023.100481, 2023.

Wei, S., Zhang, H., Xu, Z., Lin, G., Lin, Y., Liang, X., Ling, J., Wee, A. K. S., Lin, H., Zhou, Y., and Gong, P.: Coastal urbanization may indirectly positively impact growth of mangrove forests, Commun Earth Environ, 5, 608, https://doi.org/10.1038/s43247-024-01776-y, 2024.

Willemsen, P. W. J. M., Horstman, E. M., Borsje, B. W., Friess, D. A., and Dohmen-Janssen, C. M.: Sensitivity of the sediment trapping capacity of an estuarine mangrove forest, Geomorphology, 273, 189–201, https://doi.org/10.1016/j.geomorph.2016.07.038, 2016.

Wu, S., Yuan, B., Liu, S., Wang, Q., Liu, J., Yan, C., Hong, H., Pavao-Zuckerman, M. A., and Lu, H.: Urbanization-driven anthropogenic and environmental factors shape soil dissolved organic matter in mangrove ecosystems, Ecosyst. Health Sustain., 10, 0154, https://doi.org/10.34133/ehs.0154, 2024.

Wu, T., Guo, J., Li, G., Jin, Y., Zhao, W., Lin, G., Luo, F.-L., Zhu, Y., Jia, Y., and Wen, L.: Soil organic carbon contents and their major influencing factors in mangrove tidal flats: A comparison between estuarine and non-estuarine areas, Ecol Process, 14, 15, https://doi.org/10.1186/s13717-025-00581-5, 2025.

Xia, S., Song, Z., Li, Q., Guo, L., Yu, C., Singh, B. P., Fu, X., Chen, C., Wang, Y., and Wang, H.: Distribution, sources, and decomposition of soil organic matter along a salinity gradient in estuarine wetlands characterized by C:N ratio, δ^{13}C-δ^{15}N, and lignin biomarker, Glob. Change Biol., 27, 417–434, https://doi.org/10.1111/gcb.15403, 2021.

Zhang, J., Gan, S., Yang, P., Zhou, J., Huang, X., Chen, H., He, H., Saintilan, N., Sanders, C. J., and Wang, F.: A global assessment of mangrove soil organic carbon sources and implications for blue carbon credit, Nat. Commun., 15, 8994, https://doi.org/10.1038/s41467-024-53413-z, 2024.

Zhang, Z., Wang, Y., Zhu, Y., He, K., Li, T., Mishra, U., Peng, Y., Wang, F., Yu, L., Zhao, X., Zhu, L., Zhu, X., and Qin, Z.: Carbon sequestration in soil and biomass under native and non-native mangrove ecosystems, Plant Soil, 479, 61–76, https://doi.org/10.1007/s11104-022-05352-1, 2022.

Zhao, Y., Wang, X., Ou, Y., Jia, H., Li, J., Shi, C., and Liu, Y.: Variations in soil δ13C with alpine meadow degradation on the eastern qinghai–tibet plateau, Geoderma, 338, 178–186, https://doi.org/10.1016/j.geoderma.2018.12.005, 2019.